



Synthesis, Spectral Characterization, Antibacterial and Anticancer Evaluation of Novel Isoniazid based Schiff Base Ligand derived Transition Metal Complexes

M. SUGANYA^{1,2,*} and G. PUTHILIBAI²

¹Department of Chemistry, Bharathiar University, Coimbatore-641046, India

²Department of Chemistry, Sri Sairam Engineering College, Chennai-600044, India

*Corresponding author: E-mail: suganya.chem@sairam.edu.in

Received: 25 November 2023;

Accepted: 2 January 2024;

Published online: 28 February 2024;

AJC-21547

A novel isoniazid based Schiff base ligand was synthesized by the condensation of 5-acetyl-N-(adamantan-2-yl)thiophene-2-carboxamide (1 mmol) and isoniazid (1 mmol). Metal complexes were prepared by reacting the Schiff base with metal(II) chloride ($M = Ni^{2+}$, Cu^{2+} and Co^{2+}), formed the novel metal coordination compound. The synthesized ligand and metal complexes were characterized by ¹H NMR, mass spectral, UV-visible, IR & EPR spectral studies, thermogravimetric analysis, cyclic voltametry and were screened with both Gram-positive and Gram-negative bacterias to evaluate the antibacterial activity by disc diffusion method. The zone of inhibition of the antibacterial assay demonstrated that all the three metal(II) complexes are active against the four bacterias, showed increased activity with increase in concentration and is more active against *S. aureas* at all concentrations. The synthesized complexes were also evaluated for its anticancer activities, only Ni(II) and Co(II) complexes showed the moderate levels of cytotoxicity activity.

Keywords: Isoniazid ligand, Schiff base, Metal complexes, TGA, Antibacterial activity, Anticancer activity.

INTRODUCTION

Schiff bases, which are versatile ligands capable of building stable complexes with a variety of metal ions, are synthesized by condensation of primary amines and carbonyl compounds. The remarkable structural features of amino adamantane and thiophene derivatives, which present exciting possibilities for biological uses, have aroused our interest in these compounds [1-3]. Amino adamantane derivatives have demonstrated effectiveness against a range of bacteria and fungi, making them promising candidates against infections [4-6].

Thiophene derivatives, modified with different functional groups, have exhibited diverse antimicrobial properties [7]. These functional groups can influence their mode of action and effectiveness against specific microorganisms [8]. These compounds characterized by their versatile coordination properties and fascinating biological activities, have garnered substantial attention in recent years. Schiff-base metal complexes have good biological behaviour like dissecting their interactions with biomolecules, cellular uptake mechanisms and intracellular behaviour, seek more attention to researchers [9-15]. In this

study, we conduct an investigation into Schiff-base metal complexes, focusing specifically on those formed from amino adamantane and thiophene derivatives in combination with nickel(II), copper(II) and cobalt(II) as central metal ions.

EXPERIMENTAL

All the solvents and chemicals used in present work were of analytical (AR or GR) grade (Sigma-Aldrich, USA) and used without any further purification. Physical constants (m.p. °C) were determined in open capillary tubes and are uncorrected. IR spectra were recorded in KBr discs (ν_{max} in cm^{-1}) on Perkin-Elmer FT-IR (Spectrum ONE) spectrophotometer, ¹H NMR spectra on a Bruker AMX (400 MHz) spectrophotometer using DMSO-*d*₆ as solvent using TMS as an internal standard and the mass spectra were captured on a mass spectrometer Waters UPLC-TQD instrument (m/z in %).

Synthesis of 5-acetyl-N-(adamantan-2-yl)thiophene-2-carboxamide: 5-Acetylthiophene-2-carboxylic acid (1 mmol) dissolved in 10 mL of DMF was mixed to triethylamine (TEA) (3 mmol) and stirred for 15 min followed by the addition of

N-ethyl-N'-dimethylamino-propyl carbodiimide (EDCI) (1.2 mmol), 1-hydroxybenzotriazole (HOBT) (1 mmol) and adamantamine (1.2 mmol) while stirring at room temperature. A precipitate was obtained when reaction mixture was added to ice cold water. This precipitate was filtered, washed with distilled water and the solid product was vacuum dried before being placed in a desiccators (**Scheme-I**).

Synthesis of Schiff base: 5-Acetyl-N-(adamantan-2-yl)-thiophene-2-carboxamide (1 mmol) and isoniazid (1 mmol) were dissolved in 20 mL of ethanol. Acetic acid in small amount was added to the solution and after being refluxed for 3 h, the reaction mixture was chilled in the refrigerator overnight. The resultant crystals were filtered, rinsed with ice cold ethanol and finally vacuum dried (**Scheme-I**).

Synthesis of metal(II) complexes: An ethanolic solution of Schiff base ligand was added to the corresponding metal(II) chloride in a 2:1 ligand-to-metal molar ratio. The reaction mixture was refluxed for 3 h and then cooled in a refrigerator overnight. The resulting solid was filtered, washed with hexane, and finally dried under vacuum (**Scheme-I**).

RESULTS AND DISCUSSION

Characterization of Schiff base ligand: In ^1H NMR data, several chemical shifts and corresponding functional groups are observed. In spectrum, two distinct CH peaks appear at δ 7.6 ppm and 7.1 ppm, suggesting the presence of carbon atoms bonded to hydrogen in a chemical environment consistent with 2-thiophene. This indicates the involvement of 2-thiophene rings in the ligand structure. An NH peak at δ 8.0 ppm indicates the presence of a 2 $^\circ$ amide group in the ligand. Multiple CH peaks with chemical shifts at δ 2.05 ppm, 3.52 ppm and 1.43 ppm are indicative of cyclohexane rings within the ligand structure. These peaks correspond to different types of C-H environments within the cyclohexane rings suggesting the cyclic nature of Schiff base. Additionally, CH_2 peaks at δ 1.49 ppm and 1.24

ppm are observed, which further support the presence of cyclohexane rings. These peaks are associated with methylene groups within the cyclohexane rings. A CH_3 peak at δ 0.9 ppm indicated the presence of a methyl group in the ligand. Moreover, the NMR spectrum also reveals the peaks corresponding to 3-pyridine structure, particularly in a DMSO solvent. These peaks occur at δ 8.32 ppm, δ 7.63 ppm, δ 8.84 ppm and δ 9.17 ppm, suggesting the involvement of 3-pyridine moiety in the ligand. Furthermore, the carbonyl ($\text{C}=\text{O}$) groups are evident in the spectrum, with peaks at various chemical shifts such as δ 0.65 ppm and δ 0.10 ppm. These carbonyl groups may be part of amide or ketone functionalities within the ligand. Lastly, there are indications of unknown substituents in some regions of the spectrum, such as unknown α -substituents in the CH_3 group and unknown substituents from 2-furan in 2-thiophene peaks [15,16] (Fig. 1).

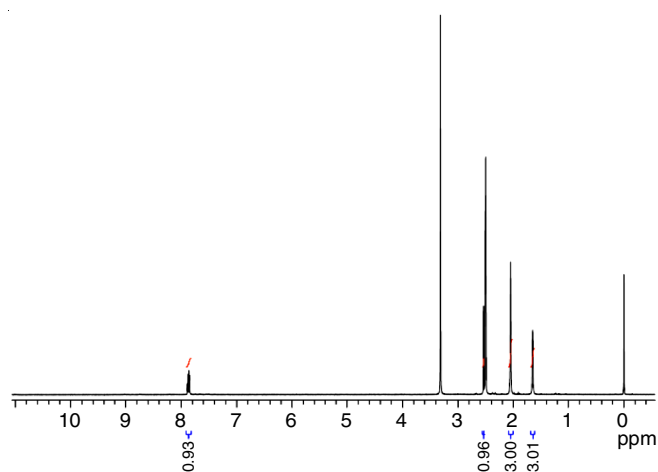
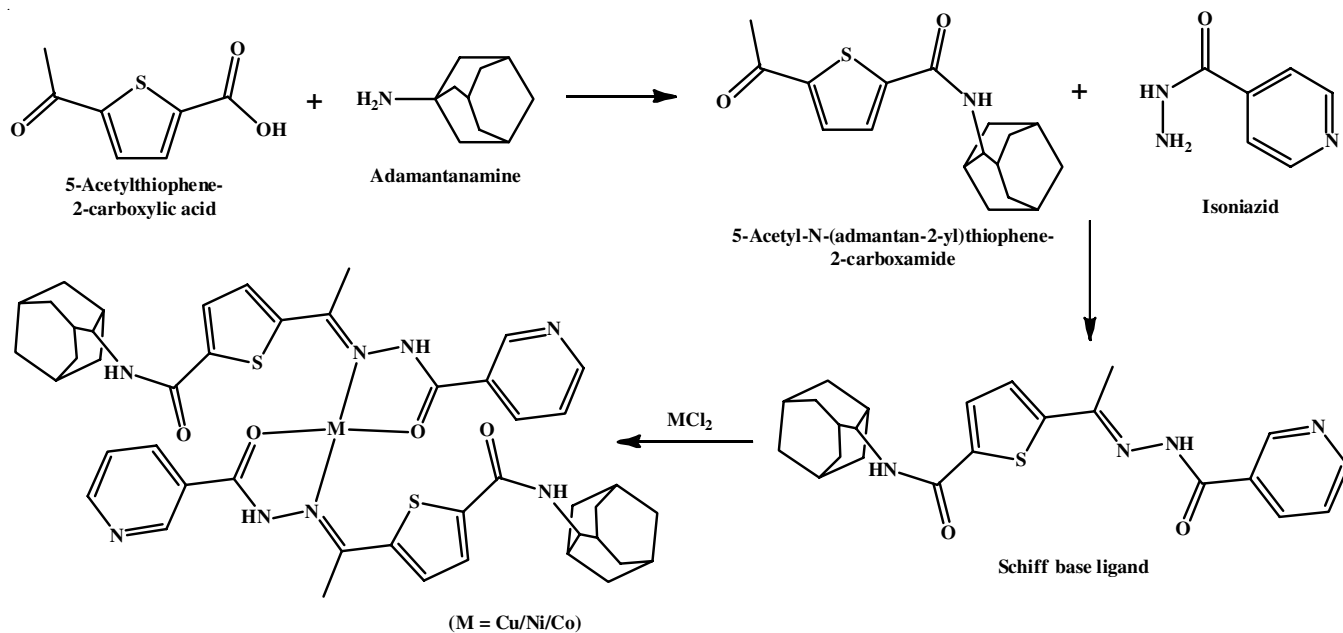


Fig. 1. Proton NMR spectra of Schiff base ligand

The mass spectra of the synthesized ligand, derived from 5-acetyl-N-(adamantan-2-yl)thiophene-2-carboxamide and



Scheme-I: Synthesis of Schiff-base metal complex of Cu, Ni and Co

isoniazid, exhibit multiple mass fragmentation peaks at m/z 423, 425, 424, 314, and 429, while the assumed molecular weight of the compound is m/z 422.54. These fragmentation peaks indicate structural modifications during the mass spectrometry process. The peak at m/z 423 suggests a minor mass gain or addition of a small fragment, while m/z 425 implies a slightly higher molecular weight. The peak at m/z 424 close to the assumed molecular weight indicates a minor mass deviation, while m/z 314 signifies significant fragmentation or loss of a substantial fragment. Finally, the peak at m/z 429 represents a higher molecular weight suggesting additional atom incorporation. These findings emphasize the necessity for structural investigation and elucidation to characterize the synthesized compound and confirmed its actual molecular composition.

Characterization of metal(II) complexes

UV visible studies: The UV-visible spectroscopy analysis conducted within the wavelength range of 200 to 1200 nm yielded critical insights into the light-absorbing properties of the ligand, copper complex, and nickel complex. The absence of any visible peaks in the UV-visible spectrum for the ligand throughout this extensive spectral range (200-1200 nm) strongly indicates that the ligand itself does not appreciably absorb light within this region. The copper(II) complex exhibited distinct absorption features, with two prominent peaks observed at 381 and 354 nm. These absorption peaks manifest the copper complex's capacity to absorb light within the UV-visible spectrum. In a similar region, the UV-Visible spectrum of the nickel(II) complex displayed a singular absorption peak at 282 nm, serving as evidence of its light absorbing properties at this particular wavelength. This absorption peak signifies that nickel(II) ions within the complex are likewise involved in electronic transitions [17-19] (Fig. 2).

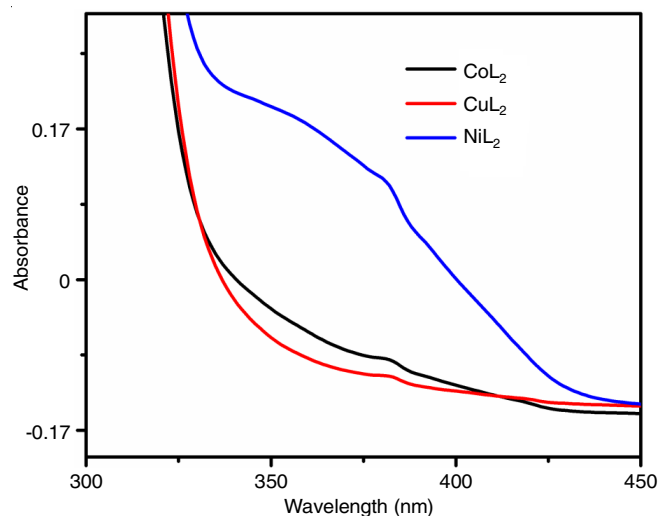


Fig. 2. UV-Visible spectra of Cu(II), Ni(II) and Co(II) complexes

IR spectral studies: The presence of peaks at 3367.91 and 1541 cm^{-1} suggests the presence of N-H bonds and N-H bending vibrations, indicating the presence of amine functional groups possibly from isoniazid. The peak at 1665.4 cm^{-1} corresponds to a carbonyl (C=O) stretching vibration indicating the

presence of a carbonyl group, which is often found in Schiff bases. Peaks at 3097.04 and 2861.71 cm^{-1} are indicative of C-H stretching vibrations, suggesting the presence of both aromatic and aliphatic hydrocarbon moieties in the molecule. The peak at 2680 cm^{-1} suggests the presence of a triple bond, which could be a carbon-carbon triple bond (C≡C). The peaks at 936 and 521 cm^{-1} could be attributed to vibrations involving sulfur (C-S) and other heteroatoms, respectively (Fig. 3a).

The changes in the IR spectrum upon complexation with Cu^{2+} , Ni^{2+} and Co^{2+} suggest that the Schiff base ligand has the potential to coordinate with these metal ions. The carbonyl (C=O) stretching vibration (16654 cm^{-1}) is particularly important, as it often shifts upon metal coordination, indicating the involvement of the carbonyl group in metal binding (Fig. 3b-d). The shifts in various peaks can provide information about the coordination modes of the ligand with the metal ions. The shifts in the N-H and C=O peaks may suggest coordination through nitrogen and oxygen atoms. The above result suggest that the synthesized metal complexes of Cu^{2+} , Ni^{2+} and Co^{2+} coordinated *via* imine group and carbonyl group and the geometry of the compounds is square planar [20,21].

Thermal studies: The thermogravimetric analysis (TGA) studies for coordinated copper(II), nickel(II) and cobalt(II) complexes revealed the distinct thermal behaviours. The coordinated copper complex exhibited a maximum normalized heat flow of 7.487 w/g at 282 °C, indicating a significant thermal event, likely associated with its unique composition and chemical properties. Similarly, coordinated nickel(II) complex displayed a notable peak with a maximum heat flow of 5.33 w/g at 271 °C, suggestive of a specific thermal process linked to its composition. In contrast, the coordinated cobalt(II) complex exhibited a substantially higher maximum normalized heat flow of 18.00 w/g at 318 °C, suggesting a more intricate and energetic thermal event, possibly due to a different ligand-metal interaction or composition (Fig. 4a-b).

The TGA analysis results for coordinated copper, nickel, and cobalt complexes revealed the distinctive thermal behaviours. The maximum temperature differences observed at 500 °C for copper (3.243 °C), 433 °C for nickel (3.290 °C) and 457 °C for cobalt (3.791 °C) signify significant thermal events in each complex (Fig. 4b) [22,23].

Electrochemical studies: The electrochemical behaviour of coordinated copper(II) complex can be analyzed based on the cyclic voltammetry (CV) data includes the reduction and oxidation peaks at specific voltages. The presence of two reduction peaks indicates that the coordinated copper(II) complex undergoes two distinct reduction processes. The reduction peak at 0.6482 V corresponds to a more difficult-to-reduce species in the complex. This could involve the reduction of the copper ion itself or a ligand that requires a higher energy input to become reduced. The reduction peak at 0.00784 V represents an easier-to-reduce species within the complex. The proximity of the oxidation potential (0.6353 V) to one of the reduction peaks (0.6482 V) suggests that the redox processes in this complex are relatively close in energy, which can be indicative of a reversible or quasi-reversible redox behaviour (Fig. 5).

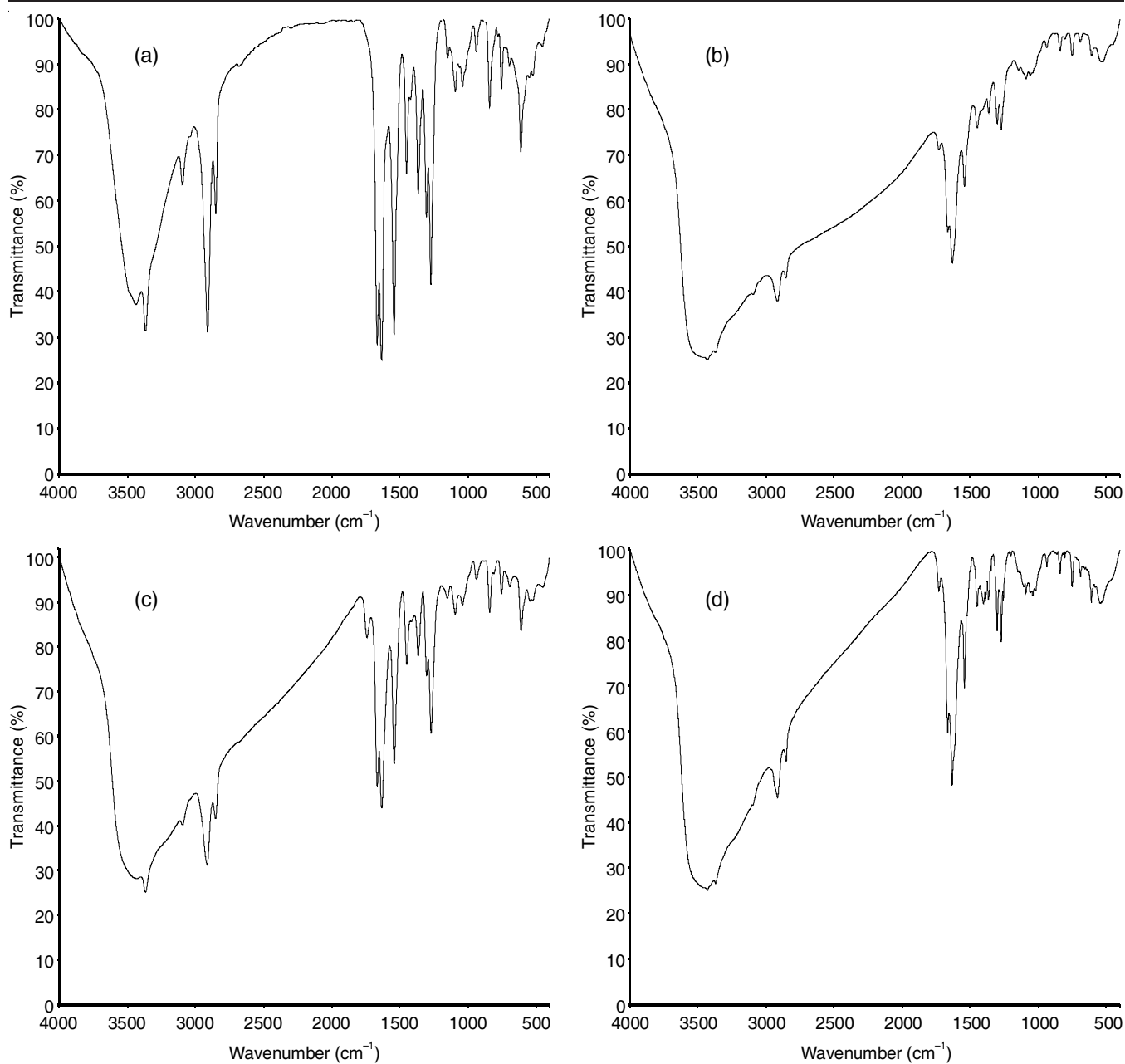


Fig. 3. IR spectra of (a) Schiff base ligand, (b) Cu complex, (c) Ni complex and (d) Co complex

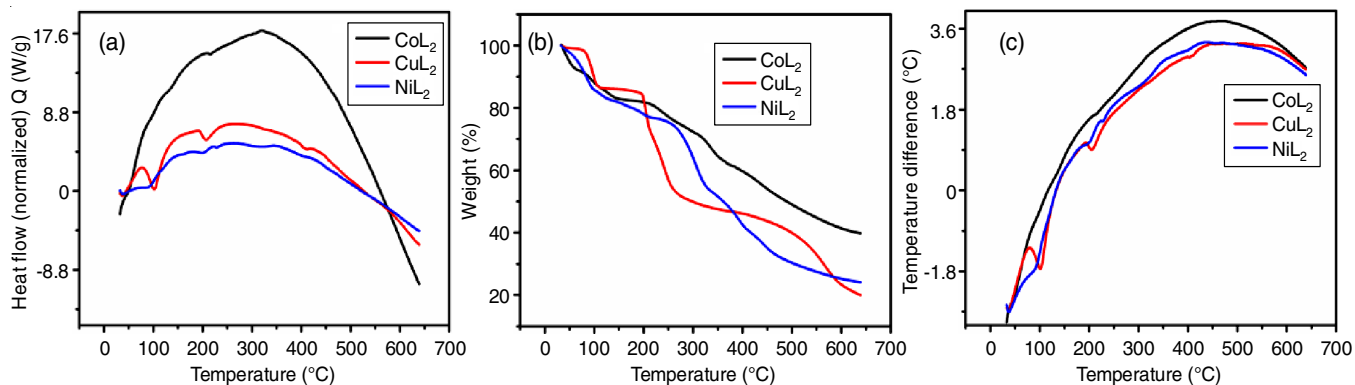


Fig. 4. Thermogravimetric analysis of metal complexes of copper, nickel and cobalt coordinated by Schiff base ligand; (a) temperature and weight percentage, (b) temperature and normalized heat flow and (c) temperature and temperature difference

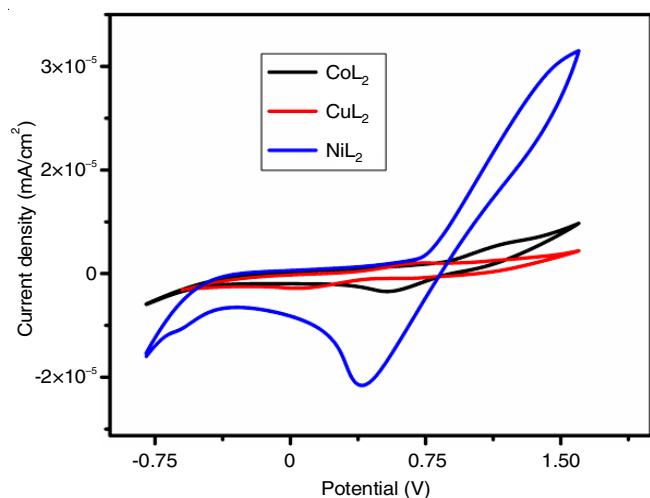


Fig. 5. Electrochemical studies of metal complexes of copper, nickel and cobalt coordinated by Schiff base ligand in three electrode system

The reduction peak obtained for nickel(II) complex at 0.4066 V suggests that the complex is capable of accepting electrons at this potential. In a square planar coordination environment, the nickel ion is typically coordinated by four ligands in a flat, square arrangement. The reduction process may involve the reduction of nickel ion or one of the coordinated ligands. The oxidation peak at 1.1686 V indicates that the complex can lose electrons at this potential. Similar to the reduction process, the oxidation process may involve the oxidation of the nickel ion or one of the coordinated ligands. The relatively high oxidation potential suggests that the oxidation process requires a significant energy input, indicating that the complex has a tendency to remain in a reduced state under typical electrochemical conditions.

The obtained cyclic voltammetry (CV) data indicates that the coordinated square planar cobalt(II) complex undergoes a reduction peak at 0.5494 V and an oxidation peak at 1.1439 V. The reduction peak at 0.5494 V suggests that the complex is capable of accepting electrons at this potential. In a square

planar coordination environment, the cobalt ion is typically coordinated by four ligands arranged in a flat, square arrangement. The reduction process may involve the reduction of the cobalt ion or one of the coordinated ligands. The oxidation peak at 1.1439 V indicates that the complex can lose electrons at this potential. Similar to the reduction process, the oxidation process may involve the oxidation of the cobalt ion or one of the coordinated ligands. The relatively high oxidation potential suggests that the oxidation process requires a significant energy input indicating that the complex has a tendency to remain in a reduced state under typical electrochemical conditions [24,25].

ESR spectral analysis: The *g*-value is a dimensionless quantity that expresses the ratio of the magnetic field experienced by an electron to the strength of the applied magnetic field. In case of copper(II) complex, the measured *g*-value of 2.8512 stands out significantly from the typical *g*-value of approximately 2.0023 associated with free electrons. This substantial deviation underscores the distinctive electron environment within the complex. The specific *g*-value of 2.8512 suggests that the unpaired electron(s) in the complex encounter a magnetic milieu distinct from that of free electrons. This divergence can be attributed to the intricate influence of the copper ion's coordination environment and the ligands surrounding it. In general, the observed *g*-value acts as a fingerprint of the complex's unique electron structure and the interactions taking place within its coordination sphere. The magnetic field at which resonance occurs (310.348 mT) is an experimental parameter that indicates the strength of the applied magnetic field required to achieve resonance. A higher magnetic field is typically associated with species that have higher energy differences between their spin states. The ESR results (Fig. 6) suggest that the coordinated copper(II) complex contains paramagnetic species with an electron environment significantly different from that of free electrons (*g* = 2.0023). The unique *g*-value of 2.8512 indicates a distinct electronic structure within the complex, likely influenced by the coordination of copper with ligands. Additionally, the relatively high magnetic field of 310.348 mT

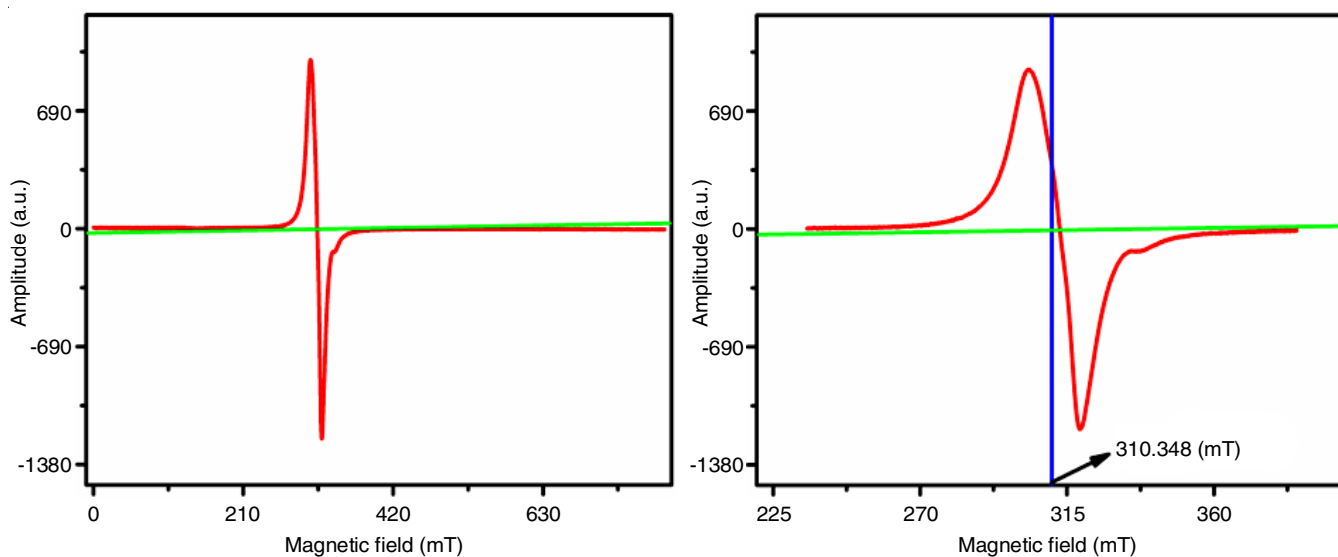


Fig. 6. ESR studies of metal complexes of copper, coordinated by Schiff base ligand

indicates a significant energy separation between electron spin states within the complex.

From the results of UV-Visible, IR, CV and ESR studies the synthesized metal complexes of Cu, Ni and Co coordinated via imine group and carbonyl group and the geometry of the compounds is square planar [26,27].

Antibacterial studies: The antibacterial studies of the synthesized compounds against different bacterial strains under various concentrations was analyzed. Table-1 shows the results of an antibacterial assay using different compounds at various concentrations (500, 1000 and 2000 µg) against four different bacteria (*S. aureus*, *B. subtilis*, *E. coli* and *P. aeruginosa*) as indicated by the zone of inhibition (mm). The ligand did not show any inhibitory activity against any of the tested bacteria, whereas cobalt(II) complex showed the moderate inhibitory activity against all bacteria except *P. aeruginosa*. The zone of inhibition generally increased with higher concentrations. The copper(II) complex also displayed the inhibitory activity against all the tested bacteria and the inhibitory activity increased with higher concentrations. In case of nickel(II) complex, the complex also showed the inhibitory activity against some bacteria, but not all. Overall, the copper(II) complex exhibited the most significant inhibitory activity across a wide range of concentrations and against multiple bacterial strains.

Anticancer studies: The results of the cell viability assay reveal varying degrees of cytotoxicity among the tested compounds are shown in Fig. 7. The copper(II) complex displayed the strongest inhibitory effect, causing a substantial reduction in cell viability at a concentration of 10.95 µg, indicating its potent cytotoxic properties. Cisplatin, the reference standard, exhibited the similar high cytotoxicity, further validating its well-known role as a potent cytotoxic agent. The nickel(II)

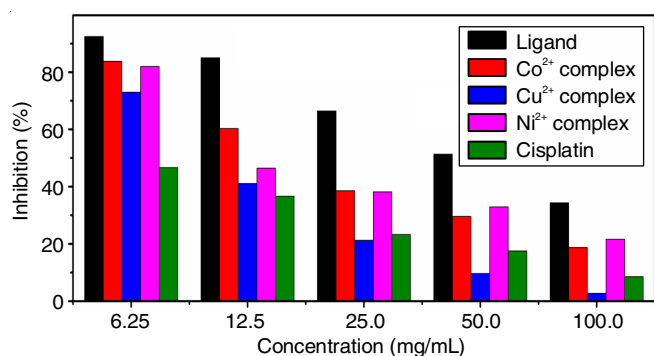


Fig. 7. Anticancer studies of metal complexes of copper, nickel and cobalt of Schiff base

and cobalt(II) complexes showed the intermediate levels of cytotoxicity, moderately inhibiting cell growth at their respective concentrations. In contrast, to Schiff base ligand had the mildest impact on cell viability, with more than half of the cells remaining viable at a concentration of 52.17 µg. These results underscore the varying cytotoxic potentials of the compounds and provide insights into their potential applications in the context of cell growth and proliferation inhibition [28,29] (Fig. 7).

Conclusion

In this study, 5-acetyl-N-(adamantan-2-yl)thiophene-2-carboxamide was successfully synthesized and used to form a Schiff base. Metal(II) complexes (Cu²⁺, Co²⁺ and Ni²⁺) of the Schiff base ligands were then prepared by reacting the Schiff base with metal(II) chlorides, demonstrating the development of novel metal coordination compounds. The study evaluated the antibacterial activity using a disc diffusion method and assessed the anticancer potential of synthesized compounds through a cell viability assay, revealing their bioactive properties against microbial species and *in vitro* cytotoxicity. The UV-Visible studies elucidated the light absorbing capabilities of copper(II) and nickel(II) complexes, showcasing their distinct electronic transitions. IR spectral studies identified functional groups and indicated the ligand-metal coordination, with shifts in peaks suggesting the varying coordination modes. Thermogravimetric analysis unveiled unique thermal behaviours, while the electrochemical studies unveiled redox processes within the metal(II) complexes. ESR spectral analysis provided a glimpse into the electron environment within the copper(II) complex. The antibacterial assay demonstrated the copper(II) complex's potent inhibitory activity, especially against *P. aeruginosa*, while the anticancer assay highlighted varying degrees of cytotoxicity among the compounds. Overall, copper(II) complex emerged as a promising candidate with significant antibacterial and anticancer potential, underscoring its suitability for further exploration in the biomedical applications.

CONFLICT OF INTEREST

The authors declare that there is no conflict of interests regarding the publication of this article.

REFERENCES

1. A. Bessette and G.S. Hanan, *Chem. Soc. Rev.*, **43**, 3342 (2014); <https://doi.org/10.1039/C3CS60411J>

TABLE-1
ANTIBACTERIAL ACTIVITY OF LIGAND AND METAL COMPLEXES

Samples	Zone of Inhibition (mm)											
	<i>S. aureus</i>			<i>B. subtilis</i>			<i>E. coli</i>			<i>P. aeruginosa</i>		
	500 µg	1000 µg	2000 µg	500 µg	1000 µg	2000 µg	500 µg	1000 µg	2000 µg	500 µg	1000 µg	2000 µg
Nicotinohydrazide – ligand	–	–	–	–	–	–	–	–	–	–	–	–
Cobalt complex	10	16	20	10	14	20	8	14	18	10	14	18
Copper complex	8	10	14	8	10	14	16	20	24	8	10	14
Nickel complex	9	12	18	–	10	12	–	8	14	–	10	14
Streptomycin (20 µg)		24			22			24			22	

2. E.V. Suslov, K. Yu Ponomarev, K.P. Volcho and N.F. Salakhutdinov, *Russ. J. Bioorg. Chem.*, **47**, 1133 (2021); <https://doi.org/10.1134/S1068162021060236>
3. J.M. Cameron, G. Guillemot, T. Galambos, S.S. Amin, E. Hampson, K.M. Haidaraly, G.N. Newton and G. Izzet, *Chem. Soc. Rev.*, **51**, 293 (2022); <https://doi.org/10.1039/D1CS00832C>
4. A. Ragab, M.S. Abusaif, D.S. AboulMagd, M.M.S. Wassel, G.A.M. Elhagali and Y.A. Ammar, *Drug Dev. Res.*, **83**, 1305 (2022); <https://doi.org/10.1002/ddr.21960>
5. G. Puthilibai, S. Vasudhevan, S.K. Rani and G. Rajagopal, *Spectrochim. Acta A Mol. Biomol. Spectrosc.*, **72**, 796 (2009); <https://doi.org/10.1016/j.saa.2008.11.019>
6. D.B. Shinde, R. Pawar, J. Vitore, D. Kulkarni, S. Musale and P.S. Giram, *Polym. Adv. Technol.*, **32**, 4204 (2021); <https://doi.org/10.1002/pat.5457>
7. R. Shah and P.K. Verma, *Chem. Cent. J.*, **12**, 137 (2018); <https://doi.org/10.1186/s13065-018-0511-5>
8. T. Boibessot, C.P. Zschiedrich, A. Lebeau, D. Bénimèlis, C. Dunyach-Remy, J.P. Lavigne, H. Szurmant, Z. Benfodda and P. Meffre, *J. Med. Chem.*, **59**, 8830 (2016); <https://doi.org/10.1021/acs.jmedchem.6b00580>
9. G. Puthilibai, V. Devatarika, B. Haewon, S.S. Behura, H.K. Lautre, V. Subha, P. Sangwan and J. Sunil, *Bull. Chem. Soc. Ethiop.*, **37**, 1133 (2023); <https://doi.org/10.4314/bcse.v37i5.6>
10. B. Englinger, C. Pirker, P. Heffeter, A. Terenzi, C.R. Kowol, B.K. Keppler and W. Berger, *Chem. Rev.*, **119**, 1519 (2018); <https://doi.org/10.1021/acs.chemrev.8b00396>
11. M.R. Slobodian, J.D. Petahtegoose, A.L. Wallis, D.C. Levesque and T.J. Merritt, *Toxics*, **9**, 269 (2021); <https://doi.org/10.3390/toxics9100269>
12. G. Puthilibai, S. Vasudhevan, S. John Mary, *Mater. Today: Proc.*, **36**, 809 (2021); <https://doi.org/10.1016/j.matpr.2020.07.008>
13. P. Ghanghas, A. Choudhary, D. Kumar and K. Poonia, *Inorg. Chem. Commun.*, **130**, 108710 (2021); <https://doi.org/10.1016/j.inoche.2021.108710>
14. G. Puthilibai, A. Lazha, T. Pushpa Malini, S. Chitra Devi, V. Devatarika and S. Vasudhevan, *AIP Conf. Proc.*, **2464**, 040003 (2022); <https://doi.org/10.1063/5.0083319>
15. O.Q. Munro, S.D. Strydom and C.D. Grimmer, *New J. Chem.*, **28**, 34 (2004); <https://doi.org/10.1039/B305946D>
16. C. Fabbro, S. Armani, L.-E. Carloni, F. De Leo, J. Wouters and D. Bonifazi, *Eur. J. Org. Chem.*, **2014**, 5487 (2014); <https://doi.org/10.1002/ejoc.201402654>
17. M.A. Hadi and I.K. Kareem, *Res. J. Adv. Sci.*, **1**, 1 (2020); <https://doi.org/10.6084/rjas.v1i1.251>
18. G. Puthilibai, S. Vasudhevan and G. Rajagopal, *Acta Crystallogr.*, **E64**, o1333 (2008); <https://doi.org/10.1107/S1600536808017443>
19. M.A. Manan and M.F. Mohammad, *Trends in Sciences*, **19**, 23 (2022); <https://doi.org/10.48048/tis.2022.1500>
20. M. Pervaiz, S. Sadiq, A. Sadiq, U. Younas, A. Ashraf, Z. Saeed, M. Zuber and A. Adnan, *Coord. Chem. Rev.*, **447**, 214128 (2021); <https://doi.org/10.1016/j.ccr.2021.214128>
21. A. Afrin and P.C. Swamy, *Coord. Chem. Rev.*, **494**, 215327 (2023); <https://doi.org/10.1016/j.ccr.2023.215327>
22. M.S. Refat, M.Y. El-Sayed and A.M. Adam, *J. Mol. Struct.*, **1038**, 62 (2013); <https://doi.org/10.1016/j.molstruc.2013.01.059>
23. Y. Song, Z. Xu, Q. Sun, B. Su, Q. Gao, H. Liu and J. Zhao, *J. Coord. Chem.*, **61**, 1212 (2008); <https://doi.org/10.1080/00958970701509768>
24. A.A. Al-Riyaahee, H.H. Hadadd and B.H. Jaaz, *Orient. J. Chem.*, **34**, 2927 (2018); <https://doi.org/10.13005/OJC%2F340632>
25. M. Kuate, M.A. Conde, E. Ngandung Mainsah, A.G. Paboudam, F.M. Tchieno, K.I. Ketchemen, I. Tonle Kenfack and P.T. Ndifon, *J. Chem.*, **2020**, 5238501 (2020); <https://doi.org/10.1155/2020/5238501>
26. V.P. Singh, *Spectrochim. Acta A Mol. Biomol. Spectrosc.*, **71**, 17 (2008); <https://doi.org/10.1016/j.saa.2007.11.004>
27. S. Chandra and Sangeetika, *Spectrochim. Acta A Mol. Biomol. Spectrosc.*, **60**, 147 (2004); [https://doi.org/10.1016/S1386-1425\(03\)00220-8](https://doi.org/10.1016/S1386-1425(03)00220-8)
28. K. Venkateswarlu, N. Ganji, S. Daravath, K. Kanneboina and K. Rangan, *Polyhedron*, **171**, 86 (2019); <https://doi.org/10.1016/j.poly.2019.06.048>
29. J. Devi, S. Sharma, S. Kumar, B. Kumar, D. Kumar, D.K. Jindal and S. Das, *Appl. Organomet. Chem.*, **36**, 6760 (2022); <https://doi.org/10.1002/aoc.6760>